



Effect of Transglutaminase on Structure and Gelation Properties of Mung Bean Protein Gel

Rui-Xue Wang¹ · Ying-Qiu Li¹ · Gui-Jin Sun¹ · Chen-Ying Wang¹ · Yan Liang¹ · Dong-Liang Hua² · Lei Chen² · Hai-Zhen Mo³

Received: 18 January 2023 / Accepted: 20 March 2023 / Published online: 28 March 2023
© The Author(s), under exclusive licence to Springer Science+Business Media, LLC, part of Springer Nature 2023

Abstract

The aim of this study was to investigate the effect of transglutaminase (TGase) treatment on structure and gelation properties of mung bean protein gel (MBPG). Structure properties for MBPG were determined by surface hydrophobicity, free sulfhydryl groups, sodium dodecyl sulfate polyacrylamide gel electrophoresis (SDS-PAGE), Fourier transform infrared spectra (FTIR), intermolecular forces and scanning electron microscopy (SEM). And the gelation properties of MBPG were characterized by rheological properties, textural properties, and water holding capacity (WHC). TGase treatment reduced surface hydrophobicity and free sulfhydryl group content of MBPG. SDS-PAGE showed that TGase cross-linking caused the protein band of TGase-induced MBPG to become shallow or disappear, especially 50.1 kDa band. In addition, TGase treatment changed the secondary structure of MBPG, with a reduction in β -sheet and an increase in β -turn and random coil. Intermolecular forces analysis manifested that covalent cross-linking and disulfide bonds were the primary forces involved in TGase-induced MBPG, and TGase treatment limited non-covalent interactions. SEM images indicated that the network structure of TGase-induced MBPG was more compact with smaller and more uniform pores than that of the control, especially at 30 U/g. Compared with the control, storage modulus (G'), hardness, chewiness, springiness, cohesiveness and WHC of 30 U/g TGase-induced MBPG reached the maximum of 45537 Pa, 1337.59 g, 1111.43, 0.99, 0.93, 87.0%, respectively. The results of this study showed that TGase treatment was a reliable method to improve the gelation properties of MBPG, especially at 30 U/g.

Keywords Mung bean protein gel · Transglutaminase · Structure properties · Gelation properties

Introduction

As the world population grows, there is increasingly the consumption of animal protein for human beings in the food industry. But the production of animal protein increases the demand for land resources and greenhouse gas emissions, so limits the availability of animal protein [1]. To meet this

challenge, the application of plant protein as a substitute for animal protein is increasing all over the world, such as soybean protein, peanut protein, pea proteins and mung bean protein (MBP) [2]. MBP has abundant essential amino acids, such as lysine, leucine, phenylalanine and valine, which can supply nutrients to meet the requirements of amino acid for human body [3]. On the other hand, MBP and its peptides also have many physiological activities, such as antioxidant, antiproliferation and angiotensin-converting enzyme inhibitory activities [4]. Furthermore, MBP has good solubility, water absorption, oil absorption, emulsifying and foaming properties [5, 6]. Therefore, MBP is considered to be an ideal replacement for animal proteins. Nevertheless, the application of MBP in the food industry has been limited due to its poor gel-forming ability [7]. Currently, several strategies have been developed to improve the gelation properties of proteins, including physical methods (e.g., high

✉ Ying-Qiu Li
lyq@qlu.edu.cn; sdililyq@126.com

¹ School of Food Science and Engineering, Qilu University of Technology (Shandong Academy of Sciences), No. 3501 University Road of Changqing District, Jinan 250353, China

² School of Energy and Power Engineering, Qilu University of Technology (Shandong Academy of Sciences), No. 3501 University Road of Changqing District, Jinan 250353, China

³ School of Food and Biological Engineering, Shaanxi University of Science and Technology, Xi'an 453003, China

pressure and ultrasound) [8, 9], chemical methods (e.g., ionic strength) [10] and enzymatic methods [11].

Transglutaminase (TGase, EC 2.3.2.13) is an effective and green cross-linking agent, and is one of the most commonly used enzymes for improving protein gelation [12]. Transglutaminase could catalyze the acyl transfer reaction between the γ -hydroxylamine groups of glutamine residues (Gln) and ϵ -amino groups of lysine residues (Lys), leading to inter- or intramolecular ϵ -(γ -Gln)-Lys cross-linking and the formation of isopeptide bonds between proteins [13]. TGase-induced cross-linking reactions could cause changes in molecular structure and improve the textural properties as well as water holding capacity of food proteins, including pea, wheat, soy and myofibrilla, etc. [14–17]. Jin & Zhong [14] reported that the addition of TGase improved the rheological properties of soy protein hydrogels, resulting in a stronger hydrogel formation. Yasir et al. [15] also found that TGase-treated soy protein could form a firmer tofu and more uniform network structure. Sun & Arntfield [16] stated that TGase formed cross-links between pea protein polypeptide chains, which improved the strength and elasticity of the gel. Norziah et al. [17] demonstrated that TGase-catalyzed fish gelatin polymer formed a dense and small void in the homogeneous gel network structure, significantly improving the gelling properties of fish gelatin.

Although TGase has been successfully applied to improve the gelation properties of some food protein, there is limited information on the effect of TGase on the gelation properties of mung bean protein gel (MBPG). Therefore, the aim of this study was to investigate the effect of TGase on structure and gelation properties of MBPG. Structure properties of MBPG were evaluated by surface hydrophobicity, free sulfhydryl groups, sodium dodecyl sulfate polyacrylamide gel electrophoresis (SDS-PAGE), Fourier transform infrared spectra (FTIR), intermolecular forces and scanning electron microscopy (SEM). And gelation properties including rheological properties, textural properties and WHC of MBPG were also analyzed. These results would provide a theoretical basis for the application of TGase-induced MBPG in food industry.

Materials and Methods

Materials

Peeled mung bean (containing 36% protein, 1% fat and 15% carbohydrate) was supplied by Shandong Fanpu Food Co. Ltd. (Linyi, China). Transglutaminase (TGase) with an activity of 120 U/g was purchased from Shandong Longcote Enzyme Preparation Co. Ltd. (Linyi, China). All the chemical reagents used in the experiments were of analytical grade and were bought from Sinopharm Chemical Reagent (Shanghai, China).

Preparation of Mung Bean Protein (MBP)

MBP was prepared according to the previously method described by Liu et al. [5] with slight modifications. The peeled mung beans (100 g) were ground into powder with a high-speed crusher (HX-200, Xi'an Hardware Pharmaceutical Factory, Zhejiang, China) and then sieved (100-mesh). The sieved mung bean powder (100 g) was dissolved in deionized water (1500 mL) and then adjusted the pH to 9.0 using 1.0 M NaOH. The obtained mixture was stirred continuously using a stirrer (S10-3, Shanghai Sile Instrument Co. Ltd., Shanghai, China) at 40°C for 2 h and then centrifuged at 4000 \times g for 10 min at 25°C with a centrifuge (5804R, Eppendorf AG, Hamburg, Germany) to collect the supernatant. The supernatant was adjusted to pH 4.5 (isoelectric point of protein) using 1.0 M HCl and centrifuged at 4000 \times g for 10 min at 25°C to collect the protein precipitate. The protein precipitate was washed and further centrifuged three times with deionized water. Then, the precipitate was resuspended in deionized water (1:10, w/v) and the pH was adjusted to 7.0 using 1.0 M NaOH. The obtained suspension was freeze-dried to be regarded as mung bean protein (MBP) with 87.98 \pm 1.24% purity as determined by the Kjeldahl method ($N \times 6.25$) [18].

Preparation of TGase-induced MBP Gel (MBPG)

MBP was dispersed in deionized water at a concentration of 18% (w/v) and stirred for 1 h at room temperature (25°C). TGase was mixed with 18% MBP solution to reach enzyme concentrations of 5 U/g, 10 U/g, 20 U/g, 30 U/g, 40 U/g and 50 U/g protein, respectively. The mixed solution was incubated in a water bath at 40°C for 1 h and then heated at 95°C for 30 min. After, the obtained TGase-induced MBPG immediately cooled in ice water for 10 min and stored in 4°C for 24 h to promote gel formation. The MBPG without TGase treatment was defined as control.

Surface Hydrophobicity

The surface hydrophobicity of MBPG was measured according to the method reported by Wen et al. [19]. The freeze-dried MBPG was dissolved in 0.01 M phosphate buffer (pH 7.0) and diluted to 0.05 mg/mL. 8-anilino-1-naphthalenesulfonic acid (ANS) was dissolved in 0.01 M sodium phosphate buffer (pH 7.0) to obtain 8.0 mM ANS solution. Aliquots (20 μ L) of ANS solution were mixed with 4 mL of each diluted solution and kept in the dark for 20 min. Finally, the excitation and emission wavelengths of the fluorescence spectrophotometer (F2700, Hitachi,

Tokyo, Japan) were set to 374 nm and 485 nm to determine the surface hydrophobicity of MBPG.

Free Sulfhydryl Groups

The free sulfhydryl groups content of MBPG was determined as described by Li et al. [20] with some modifications. An aliquot (50 mg) of freeze-dried MBPG was dissolved in 5 mL of Tris-Gly buffer (86 mM Tris, 90 mM glycine, 4 mM EDTA, pH 8.0) and centrifuged at 25°C, 10000×g for 10 min. The obtained supernatant (3mL) was mixed with 30 µL of the Ellman's reagent (4 mg/mL, 5,5'-dithiobis-2-nitrobenzoic acid (DTNB) dissolved in Tris-Gly buffer). The obtained mixture was incubated in the dark for 1 h, then the absorbance of mixture was measured at 412 nm. The free sulfhydryl groups content of MBPG was calculated by the equation (1) as follows:

$$SH (\mu\text{mol/g}) = \frac{73.53 \times A_{412} \times D}{C} \quad (1)$$

where 73.53 is $10^6/13600$ (13600 is the molar absorptivity of Ellman reagent), A_{412} is the absorbance of mixture at 412 nm, D is the dilution factor, and C is the MBPG concentration (mg/mL).

Sodium Dodecyl Sulfate-polyacrylamide Gel Electrophoresis (SDS-PAGE)

Protein patterns of MBPG were investigated by SDS-PAGE with a 12% separating gel and 3% stacking gel according to the method of Sun & Arntfield [16] with slight modifications. The freeze-dried MBPG (5 mg) was dissolved in 1 mL of reducing sample buffer (50 mM Tris-HCl of pH 8.0, 1% SDS, 10% glycerol, 0.02% bromophenol blue, and 1% 2-mercaptoethanol), and heated at 100°C for 3 min. Aliquots (10 µL) of treated samples and protein standard marker with molecular weight of 11-245 kDa (Beijing Solarbio Technology Co. Ltd., Beijing, China) were loaded onto the stacking gel slot. Electrophoresis was first run at 80 V on stacking gel and then at 120 V on separating gel. Following electrophoresis, the obtained gel was fixed with fixing solution (40% methanol, 10% acetic acid and 50% water) for 2 h, stained with 0.25% Coomassie Blue R-250 solution for 2 h, and decolorized with decolorizing solution (7.5% glacial acetic acid and 5.0% ethyl alcohol) until the protein band became clear.

Fourier Transform Infrared Spectroscopy (FTIR)

FTIR spectra of MBPG were measured using a FTIR spectrometer (Nicolet iS10, Thermo Fisher Scientific, Waltham, MA, USA) with reference to the method of Liang et al. [21].

Aliquots (2 mg) of freeze-dried MBPG were grinded with 198 mg KBr and then pressed into 1-2 mm thin slices. Each sample was scanned 64 times in the wave number range of 4000 cm^{-1} to 400 cm^{-1} with a resolution of 4 cm^{-1} . The secondary structure in the amide I band from 1600 cm^{-1} to 1700 cm^{-1} was analyzed using Peakfit v4.12.

Intermolecular Forces

The intermolecular forces involved in MBPG network formation were determined following the methods described by Jia et al. [22] with slight modifications. The freeze-dried MBPG (50 mg) was dispersed in 5 mL of 0.6 M NaCl (S1), 0.6 M NaCl + 1.5 M urea (S2), 0.6 M NaCl + 8 M urea (S3), and 0.6 M NaCl + 8 M urea + 0.5 M β -ME (S4), respectively. Then, the dispersions were incubated at room temperature for 1 h and centrifuged at 8000×g for 20 min. The soluble protein content of the supernatant was measured by the Lowry method using bovine serum albumin as the standard [23]. The solubility of S1, S2-S1, S3-S2, S4-S3 represented the contribution of ionic bonds, hydrogen bonds, hydrophobic interactions, and disulfide bonds, respectively.

Scanning Electron Microscopy (SEM)

The microstructure of MBPG was observed using SEM (Gemini 300, ZEISS, Oberkochen, Germany) as previously method described by Salahi et al. [24]. MBPG was cut into small cubes (3-5 mm) and then freeze-dried by a vacuum freeze dryer. The dried MBPG was adhered to an aluminum stub using a two-sided conductive adhesive tape and sprayed with gold for 45 s. SEM images of the gold-sprayed MBPG were photographed under the condition of 3 kV acceleration voltage and 200X magnification.

Rheological Properties

Rheological properties of MBP solution were measured with a rheometer (Physica MCR 302, Anton Paar GmbH, Graz, Austria) using the modified method of Patole et al. [25]. MBP solution (18%, w/v) of 2 mL was loaded onto a diameter 50 mm parallel plate and the gap was set to 1 mm. The exposed MBP solution at parallel plate edges was covered in silicone oil to avoid water evaporation during heating. The temperature sweep of MBP solution was carried out at a fixed frequency of 1 Hz and a constant strain of 1%. MBP solution was first heated from 25°C to 95°C at a rate of 5 °C/min, then kept at 95°C for 30 min, finally cooled to 25°C at 5°C/min. The storage modulus (G') and loss modulus (G'') were recorded continuously during the whole process.

Textural Properties

The textural properties of MBPG were tested with a textural analyzer (TA-XT plus, Stable Micro Systems, Godalming, England) according to the method of Yu et al. [26] with some modifications. The compression test of MBPG with 15 mm diameter and 10 mm height was carried out using a cylindrical probe (P/36R). The parameters were set as follows: 5.0 mm/s pre-test and post-test speed, 1.0 mm/s test speed, 5 g trigger type, and 50% compression deformation. Four parameters of textural properties for MBPG were analyzed including hardness, springiness, chewiness and cohesiveness.

Water Holding Capacity (WHC)

WHC of MBPG was analyzed using the centrifugal method proposed by Fang et al. [27]. Aliquots of 2 g MBPG (5 mm × 5 mm × 5 mm cubes) were packed with filter paper and transferred to 50 mL centrifuge tube, then centrifuged at 10000×g for 10 min at 4°C. Excess water was removed, and the surfaces of MBPG were carefully dried using dry filter paper. The centrifuge tube with MBPG before and after centrifugation was weighed accurately. WHC of MBPG was expressed as the following equation (2):

$$WHC (\%) = \frac{W_2 - W_0}{W_1} \times 100 \quad (2)$$

where W_0 is the mass (g) of centrifuge tube, W_1 is the mass (g) of MBPG before centrifugation, W_2 is the total mass (g) of centrifuge tube with MBPG after centrifugation.

Statistical Analysis

All experiments were repeated at least three times, and the data were expressed as mean ± standard deviation. IBM SPSS Statistics 23 (SPSS Institute Inc., Chicago, USA) was used for one-way analysis of variance (ANOVA) and Duncan's multiple-range test to determine the significant differences ($P < 0.05$) among means. All figures were drawn using the Origin 2017 (OriginLab, MA, USA).

Results and Discussion

Surface Hydrophobicity Analysis

The surface hydrophobicity of proteins, one of the main structural characteristics, is evaluated distribution of hydrophobic groups, which is associated with protein polymerization and gel formation [28]. Fig. 1 shows the changes

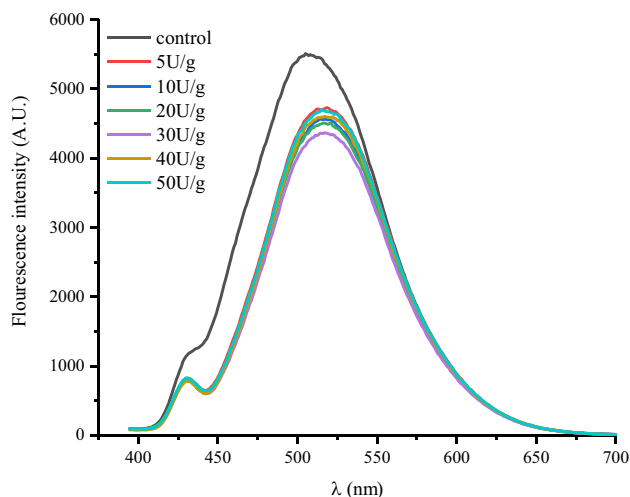


Fig. 1 Changes in surface hydrophobicity of MBPG induced by TGase

of surface hydrophobicity of TGase-induced MBPG. The surface hydrophobicity of MBPG induced by different concentrations TGase (0 U/g, 5 U/g, 10 U/g, 20 U/g, 30 U/g, 40 U/g and 50 U/g) was 5509 A.U., 4710 A.U., 4561 A.U., 4506 A.U., 4366 A.U., 4603 A.U. and 4682 A.U., respectively. These data indicated that TGase decreased the surface hydrophobicity of MBPG compared with the control. The decrease in surface hydrophobicity might be due to TGase catalyzing cross-linking among protein molecules to bury hydrophobic groups [28]. On the other hand, TGase cross-linking deaminated the hydrophobic group (such as glutamine and asparagine residues) to become glutamic acid and aspartic acid, thus reducing the surface hydrophobicity of MBPG [19]. Similarly, Nivala et al. [11] reported that TGase-induced (1000 nkat/g protein) cross-linking of faba bean protein isolate caused a reduction of surface hydrophobicity from 504 to 435 RFU. Agyare et al. [29] also observed that there was the decline in hydrophobicity of TGase treated wheat gluten hydrolysate.

Free Sulfhydryl Groups Analysis

Free sulfhydryl groups are located on the surface of protein molecules and play an important role in the formation of TGase-induced gels [30]. Fig. 2 shows the free sulfhydryl groups contents of TGase-induced MBPG. The free sulfhydryl groups contents of MBPG induced by different concentrations of TGase (0 U/g, 5 U/g, 10 U/g, 20 U/g, 30 U/g, 40 U/g and 50 U/g) were 5.235 μmol/g, 0.961 μmol/g, 0.790 μmol/g, 0.787 μmol/g, 0.775 μmol/g, 0.723 μmol/g and 0.719 μmol/g, respectively. These data showed that the free sulfhydryl groups

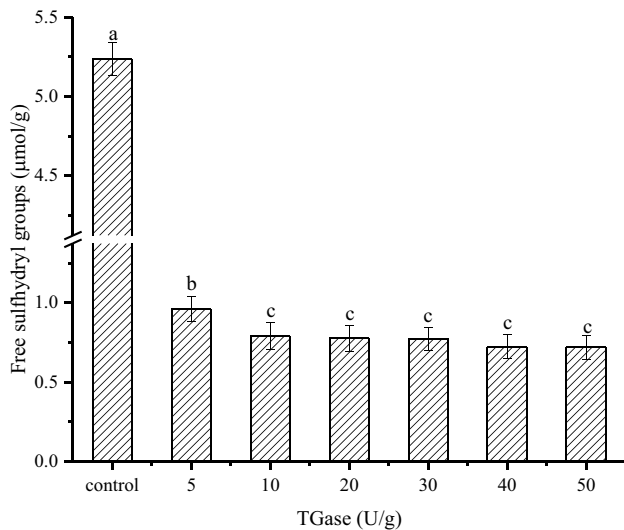


Fig. 2 Changes in free sulfhydryl groups content of MBPG induced by TGase. Data are expressed as mean ± standard deviation (*n* = 3). Different superscript letters mean significant differences between values with different TGase concentration (*P* < 0.05)

contents of MBPG decreased from 5.235 μmol/g to 0.719 μmol/g with the increase of TGase concentration from 0 U/g to 50 U/g. The decrease in free sulfhydryl groups content might be that TGase induced the free sulfhydryl groups to oxidize, forming new disulfide bonds [31]. Besides, TGase enhanced aggregation of proteins to bury some exposed free sulfhydryl groups, thus lowering the free sulfhydryl groups content [19]. Similarly, Jia et al. [22] proposed that suwari gel and kamaboko gel with TGase had lower the free sulfhydryl groups content than gel without TGase. Tang et al. [31] also found that the total sulfhydryl groups content of TGase-treated kidney protein isolate was reduced, possibly due to the formation of new disulfide bonds among exposed free sulfhydryl groups.

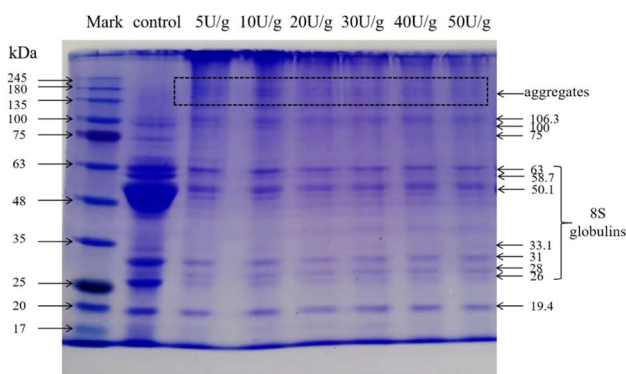


Fig. 3 Changes in SDS-PAGE profiles of MBPG induced by TGase

SDS-PAGE Analysis

SDS-PAGE was performed to confirm the degree of TGase-catalyzed covalent cross-linking of proteins in MBPG [19]. As shown in Fig. 3, the eleven protein bands in the control were located at around 19.4 kDa, 26 kDa, 28 kDa, 31 kDa, 33.1 kDa, 50.1 kDa, 58.7 kDa, 63 kDa, 75 kDa, 100 kDa and 106.3 kDa, respectively. The five main bands of 26 kDa, 31 kDa, 50.1 kDa, 58.7 kDa and 63 kDa represented the 8S globulin subunits, of which 50.1 kDa band was the most abundant. Compared with the control, the protein bands of TGase-induced MBPG became shallow or disappeared, especially the main band of 50.1 kDa, accompanied by the formation of high molecular weight polymers (>106.3 kDa). Moreover, some polymers retained in the stacking gel or did not penetrate the separating gel. These phenomena were attributed to protein aggregation following covalent cross-linking formation of glutamine and lysine reaction residues catalyzed by TGase [32]. A similar result reported that the prominent protein bands for TGase catalyzed casein-hempseed protein complex disappeared and produced a large aggregated bands in the stacking gels [32]. Fang et al. [27] also found that the myosin heavy chains band in the surimi gels with TGase almost disappeared, while the band intensity of protein near 85 kDa was increased, indicating that TGase catalyzed formation of covalent cross-linking.

FTIR Analysis

FTIR spectra are used to reflect protein conformation and the stretching vibration of functional groups [33]. Fig. 4 exhibits FTIR spectra of TGase-induced MBPG in the range of 4000–400 cm⁻¹. The peak of amide A was caused by N-H and O-H stretching vibrations at 3000–3500 cm⁻¹ to reflect

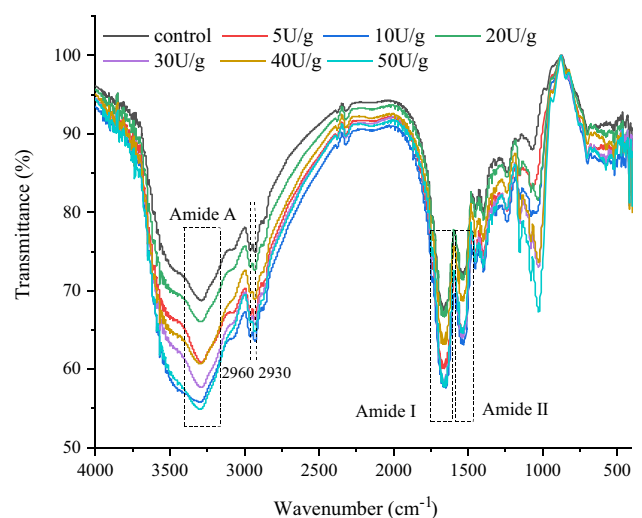


Fig. 4 Changes in FTIR spectra of MBPG induced by TGase

the strength of the hydrogen bonds in protein [34]. When N-H was involved in hydrogen bonds formation, the peak of amide A shifted to a low wavenumber [33]. The position of the amide A peak in all samples was basically the same at 3290 cm^{-1} , implying that TGase-induced MBPG did not form more hydrogen bonds. But, the amide A peak intensities (55%-66.1%) of TGase-induced MBPG were higher than that (68.7%) of the control at 3290 cm^{-1} . This result suggested that TGase catalyzed covalent cross-linking of glutamine and lysine residues to generate more amide bonds, resulting in stronger intermolecular interactions in MBPG [21]. Two peaks of 2960 cm^{-1} and 2930 cm^{-1} characterized the C-H stretching vibrations of methyl and methylene groups in proteins and lipids [5]. The two peak (2960 cm^{-1} and 2930 cm^{-1}) intensities (64.1%-73% and 64.8%-72.6%) of TGase-induced MBPG were higher than that of the control (75.1% and 74.9%), manifesting that TGase heightened the contents of methyl and methylene groups in MBPG.

The amide I band mainly was associated with the stretching vibrations of C=O and C-N, which was used to characterize protein secondary structure including α -helix, β -turn, β -sheet, and random coil [30]. The peaks of α -helix, β -turn, β -sheet, and random coil were in the range of $1650\text{--}1660\text{ cm}^{-1}$, $1660\text{--}1700\text{ cm}^{-1}$, $1600\text{--}1640\text{ cm}^{-1}$ and $1640\text{--}1650\text{ cm}^{-1}$, respectively [9]. Table 1 displays the content of protein secondary structure for TGase-induced MBPG. With increasing of TGase concentration from 0 U/g to 50 U/g, the α -helix content was almost unchanged, but the contents of β -turn and random coil increased from 30.33% to 32.41%, 22.10% to 23.95%, accompanied by the β -sheet content reduced from 27.75% to 23.37%, suggesting that TGase changed the secondary structure of MBPG. Similarly, Hu et al. [33] suggested that compared with the control group, TGase (0.02-0.08%) decreased the β -sheet content of fish gelatin- γ -polyglutamic acid, while increased the β -turn content and random coil content. Liang et al. [21] also concluded that TGase altered the secondary structure of whey protein emulsion gels. The change of protein secondary structure content of MBPG might be that TGase catalyzed covalent

cross-linking among Gln-Lys isopeptide bonds and formation of disulfide bonds to form macromolecular protein polymers [35]. Hydrogen bonds are the main force maintaining the secondary structure of proteins. The formation of these macromolecular polymers catalyzed by TGase might have effect on hydrogen bonds, including the breaking and reconnection of hydrogen bonds, thus changing the proteins secondary structure of MBPG [36]. Meanwhile, TGase caused the deamidation of asparagine and glutamine to produce aspartic acid and glutamic acid, which were important components of the β -turn structure, so increasing the β -turn content of MBPG [37]. G' , also known as the modulus of elasticity, reflects the solid-like behavior of the material and is often used to describe the springiness and hardness properties of sample [26]. It was reported that gel hardness and springiness were positively correlated with the content of β -turn, while negatively correlated with the content of α -helix [38]. Therefore, the high β -turn content resulted in the increase of hardness and springiness of TGase-induced MBPG, which was reflected in the increases in G' of TGase-induced MBPG.

The amide II band in $1500\text{ cm}^{-1}\text{--}1600\text{ cm}^{-1}$ was attributed to the stretching vibration of C-N and the bending vibration of N-H [30]. The peak intensities (63.1%-71.4%) of TGase-induced MBPG were stronger than that of the control (72.0%) at 1530 cm^{-1} , indicating that TGase increased amide bonds of MBPG [21].

Intermolecular Forces Analysis

The intermolecular forces play an important role in the gel network formation and textural properties, which are determined by the protein solubility of MBPG in different solutions [39]. Fig. 5 shows the effect of TGase on the intermolecular forces including ionic bonds, hydrogen bonds, hydrophobic interactions and disulfide bonds in MBPG. The protein solubility corresponding ionic bonds and hydrophobic interactions in MBPG decreased from 0.61% to 0.07% and 5.60% to 0.37% along with the increase of TGase

Table 1 Changes in secondary structure contents of MBPG induced by TGase

TGase (U/g)	Secondary structure composition (%)			
	α -helix	β -turn	β -sheet	Random coil
control	19.82±0.26 ^{bc}	30.33±0.36 ^d	27.75±0.56 ^a	22.10±0.37 ^b
5	19.55±0.32 ^c	31.52±0.40 ^c	25.90±0.46 ^b	23.04±0.42 ^a
10	19.72±0.22 ^c	29.94±0.45 ^d	26.60±0.39 ^b	23.73±0.46 ^a
20	20.07±0.31 ^{abc}	32.21±0.36 ^{abc}	24.27±0.33 ^c	23.45±0.49 ^a
30	20.49±0.28 ^a	32.09±0.39 ^{bc}	23.91±0.46 ^{cd}	23.50±0.56 ^a
40	19.82±0.30 ^{bc}	32.92±0.41 ^a	23.71±0.40 ^{cd}	23.55±0.52 ^a
50	20.27±0.19 ^{ab}	32.41±0.46 ^{ab}	23.37±0.26 ^d	23.95±0.46 ^a

Data are expressed as mean \pm standard deviation ($n = 3$). Different superscript letters mean significant differences between values with different TGase concentration ($P < 0.05$)

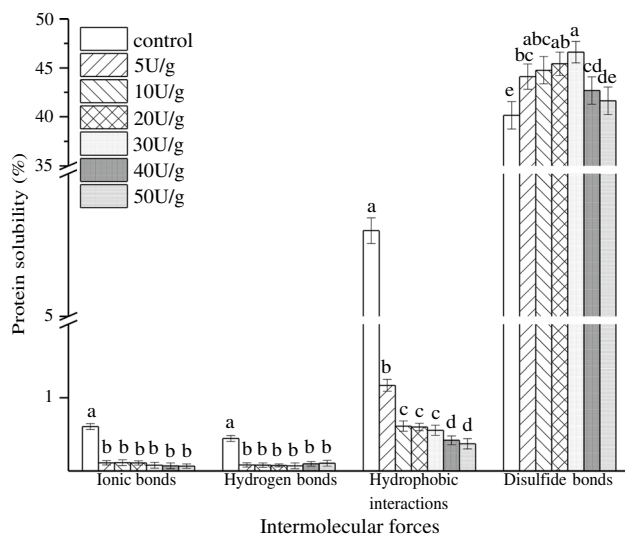


Fig. 5 Changes in intermolecular forces of MBPG induced by TGase. Data are expressed as mean \pm standard deviation ($n = 3$). Different superscript letters mean significant differences between values with different TGase concentration ($P < 0.05$)

concentration from 0 U/g to 50 U/g. The protein solubility corresponding hydrogen bonds in MBPG first lowered from 0.45% to 0.07% as TGase concentration increased from 0 U/g to 30 U/g, and then raised from 0.07% to 0.11% with the further increase of TGase concentration from 30 U/g to 50 U/g. Moreover, the protein solubility corresponding disulfide bonds added from 40.14% to 46.61% with increasing TGase concentration from 0 U/g to 30 U/g, while reduced from 46.61% to 41.63% when TGase concentration increased from 30 U/g to 50 U/g. These data indicated that MBPG network structure was mainly maintained by hydrophobic interactions and disulfide bonds, while the role of ionic bonds and hydrogen bonds was minor. Besides, TGase reduced non-covalent bonds of MBPG (including ionic bonds, hydrogen bonds and hydrophobic interactions), while increased disulfide bonds of MBPG. The reduction of non-covalent bonds in TGase-induced MBPG was due to the high binding energy and steric hindrance effect of covalent bond interactions, including cross-linking between γ -carboxamides and amino, as well as disulfide bonds [22]. Meanwhile, the cross-linking of TGase and the increase of disulfide bonds promoted the formation of macromolecular protein polymers to bury hydrophobic groups, thus weakening the hydrophobic interactions [19]. In addition, TGase could also catalyze the deamidation of hydrophobic residues glutamine to produce glutamic acid, thus reducing the hydrophobic interactions [40]. The increase of disulfide bonds content in TGase-induced MBPG might be ascribed to the cross-linking of free sulfhydryl groups by TGase to form disulfide bonds [31]. However, excessive TGase concentrations led to stronger aggregation of proteins and burial of some exposed

free sulfhydryl groups, thus reducing disulfide bonds [41]. Similarly, Wen et al. [19] noted that TGase weakened soluble proteins associated with ionic bonds, hydrogen bonds and hydrophobic interactions in apricot kernel protein concentrates gels, probably due to glutamate bond cross-linking and disulfide bonds formation. Eissa & Khan [42] also showed that TGase caused cross-linking reaction between glutamine and lysine residues creating ϵ -(γ -glutamyl) lysine bonds, which effectively limited formation of hydrophobic interactions.

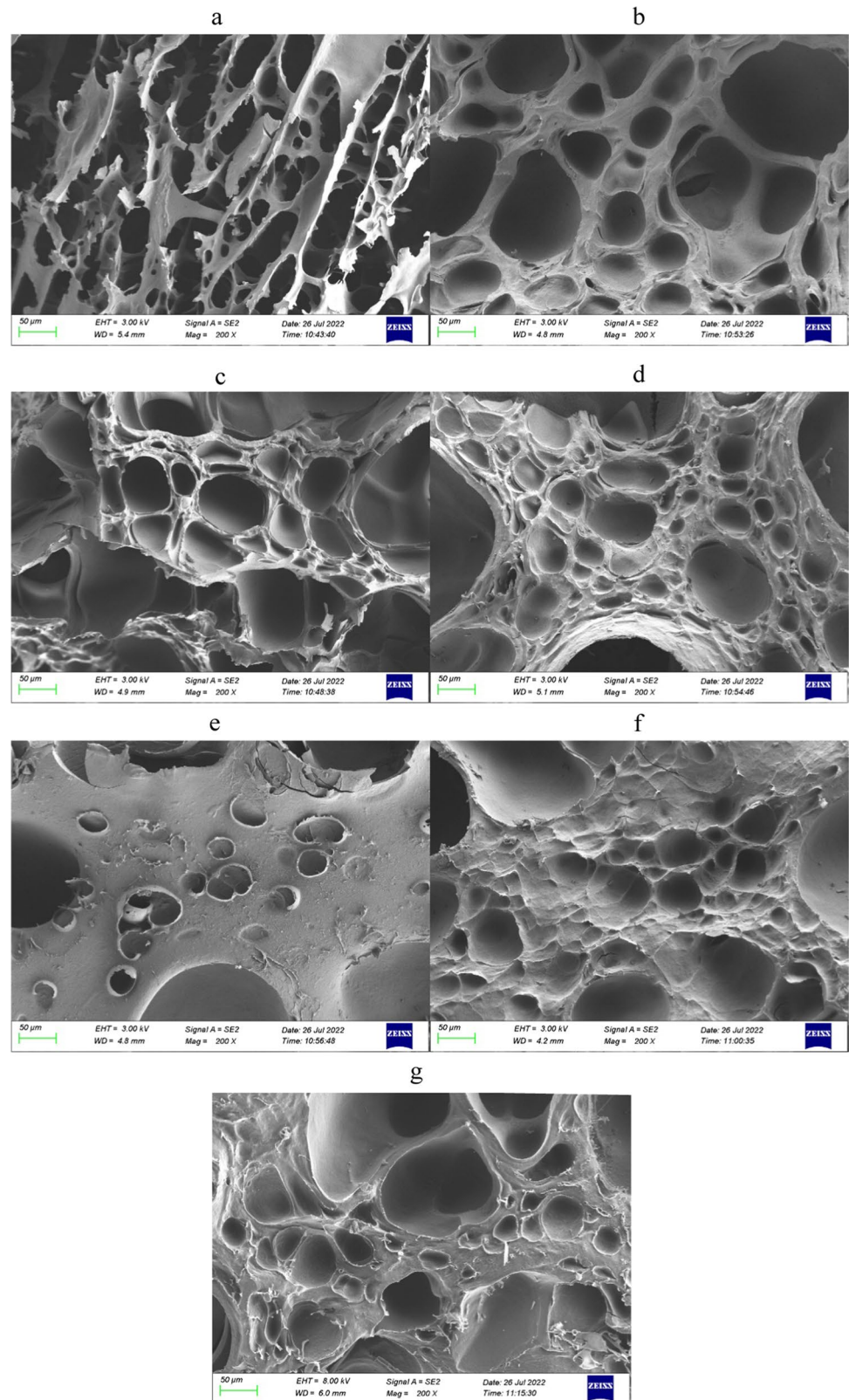
SEM Analysis

SEM can visually display the three-dimensional network structure including surface roughness, pore size and distribution of protein gel [8]. SEM images of TGase-induced MBPG are illustrated in Fig. 6. The control had honeycomb network with large and irregular pores (Fig. 6a), which was characterized by poor hardness and WHC (As shown in Fig. 8 and Fig. 9). Compared with the control, TGase-induced MBPG had more compact network with smaller and more uniform pores and smoother surface (Fig. 6b-g), especially MBPG induced by 30 U/g TGase, which was in accordance with higher hardness and WHC (As shown in Fig. 8 and Fig. 9). It was reported that TGase could catalyze ϵ -(γ -glutamyl) lysine cross-linking of protein molecules to enhance MBPG network structure [43]. The enhancement of TGase-induced MBPG network structure might also be due to the formation of many intermolecular disulfide bonds in MBPG during TGase induction [8]. Additionally, TGase might result in the formation of insoluble proteins to promote insoluble protein aggregation, which likely had a positive effect on the network structure of MBPG [19]. However, too strong TGase concentration led to excessive cross-linking of protein molecules to damage the homogeneity of MBPG network, thus enlarging the pores of MBPG network structure [32]. Similarly, Qian et al. [44] reported that the network of silver carp myofibril protein gel adding TGase (5 U/g and 10 U/g) was denser and more uniform than that of the control, indicating that TGase facilitated protein-protein interactions. Moreover, Chen et al. [45] found that camel milk acid gel prepared from 30 U/g TGase displayed a dense structure with the smallest pores.

Rheological Properties Analysis

G' is the stored energy of elastic deformation during gel formation to reflect the solid property and is generally used as an indicator of gel hardness [39]. G'' is the lost energy of viscous deformation during gel formation to reflect the liquid property. The effect of TGase on G' and G'' of MBPG during the whole process of gel formation is shown in Fig. 7a, 7b. The G' values of all samples were always higher than that of

Fig. 6 Changes in microstructure of MBPG induced by TGase. **a**: control; **b**: 5 U/g; **c**: 10 U/g; **d**: 20 U/g; **e**: 30 U/g; **f**: 40 U/g; **g**: 50 U/g



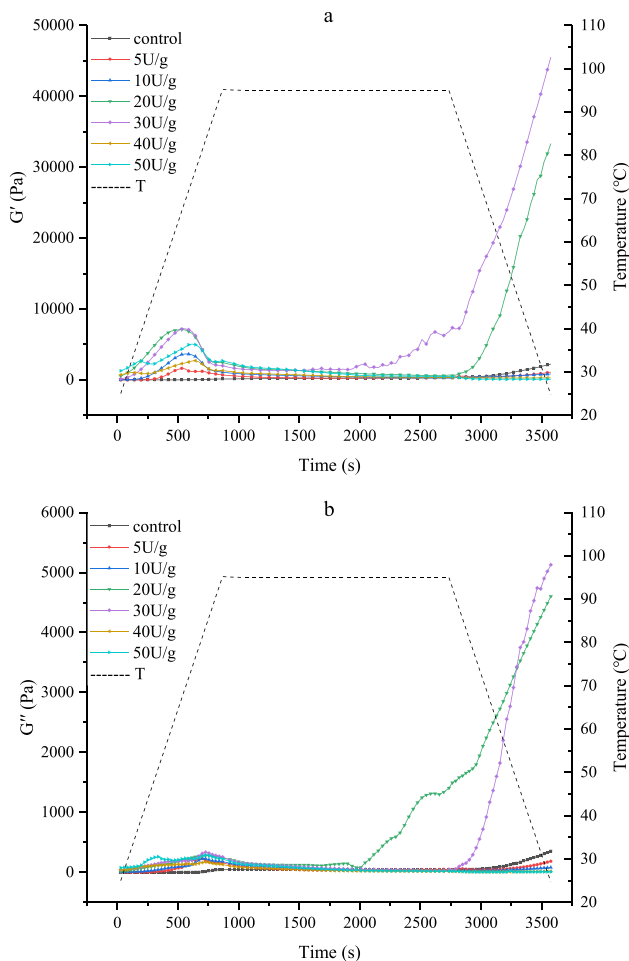


Fig. 7 Changes in rheological properties of MBP solution induced by TGase during gelation. **(a):** Change of storage modulus (G') of MBPG with temperature sweep; **(b):** Change of loss modulus (G'') of MBPG with temperature sweep

G'' values, indicating solid gel formation. Therefore, only G' value was discussed in detail as follow.

At the heating stage (25–95°C), the G' value of the control increased from 0.033 Pa to 112.94 Pa in time period of 0–868 s. At 25–70°C, the G' value of TGase-induced MBPG increased sharply from 0.617–1269.2 Pa to 1538.3–7199.6 Pa in the time period of 0–560 s, reaching a maximum value at approximately 70°C. But at 70–95°C, the G' decreased rapidly from 1538.3–7199.6 Pa to 673.28–2665.6 Pa in the time period of 560–868 s. Fang et al. also reported that the G' value of surimi gel with TGase reached the peak value at approximately 70°C [27]. The reason for the increase of G' value in the control was that heating promoted denaturation and unfolding of MBP to expose hydrophobic groups (such as glutamine and asparagine residues), thereby enhancing hydrophobic interactions to accelerate the development of the gel network structure [46]. The sharp increase of G' values of TGase-induced MBPG at 25–70°C was associated

with the covalent cross-linking of exposed glutamine and amino groups catalyzed by TGase to form the stronger gel network [22]. High temperature (70–95°C) terminated the ability of TGase to catalyze cross-linking and reduced G' value of MBPG, because protein cross-linking required low temperature to produce elastic structures. Similarly, Luo et al. [39] demonstrated that TGase catalyzed the formation of covalent cross-linking among protein molecules, thus enhancing the elasticity (G') and firmness of soy protein isolate emulsion gels.

At the insulation stage (95°C), the G' value of the control continuously increased further from 112.94 Pa to 144.67 Pa in time period of 868–2692 s, possibly because of the formation of a large number of disulfide bond [22]. However, the G' value of TGase-induced MBPG further decreased from 673.28–2665.6 Pa to 273.38–589.89 Pa in the time period of 868–2692 s. This was because although high temperature led to the formation of disulfide bonds, it destroyed the covalent crosslinking catalyzed by TGase, which played a major role in the gel network, thereby reducing the G' value of MBPG [47].

Finally, at the cooling stage (95–25°C), the G' value of MBPG induced by 0 U/g, 5 U/g, 10 U/g, 20 U/g and 30 U/g went up again sharply from 144.67–6257 Pa to 1082.1–45537 Pa in time period of 2692–3575 s. But the G' values of MBPG induced by 40 U/g and 50 U/g also gradually reduced from 349.07–465.61 Pa to 279.64–92.651 in time period of 2692–3575 s. These data indicated that low TGase concentrations increased G' value of MBPG, while excessive TGase concentrations decreased G' value of MBPG at the cooling stage. The increase of G' value in TGase-induced MBPG was related to the further cross-linking of protein molecules catalyzed by TGase during cooling [47]. However, excessive TGase cross-linking caused bond damage within the gel network and the formation of heterogeneous structures, leading to a decrease in G' value of MBPG [39]. At the end of cooling stage, the G' end value generally represents the elasticity of the finally formed gel [48]. There was the highest G' end value of MBPG induced by 30 U/g TGase, indicating 30 U/g TGase-induced MBPG had the maximum elasticity, which was consistent with the results of textural properties analysis. Similarly, Sun & Arntfield [47] reported that the continued cross-linking among protein molecules led to the increase of G' value during cooling of heat-induced chicken myofibrillar protein isolate gels with TGase (2–12 U), thus enhancing the gel hardness.

Textural Properties Analysis

Textural properties tests reflect the gelation properties and mouthfeel of gel products by simulating the effect of the tongue and teeth on the gel [49]. The changes in textural properties including hardness, chewiness, springiness, and cohesiveness of TGase-induced MBPG are summarized in

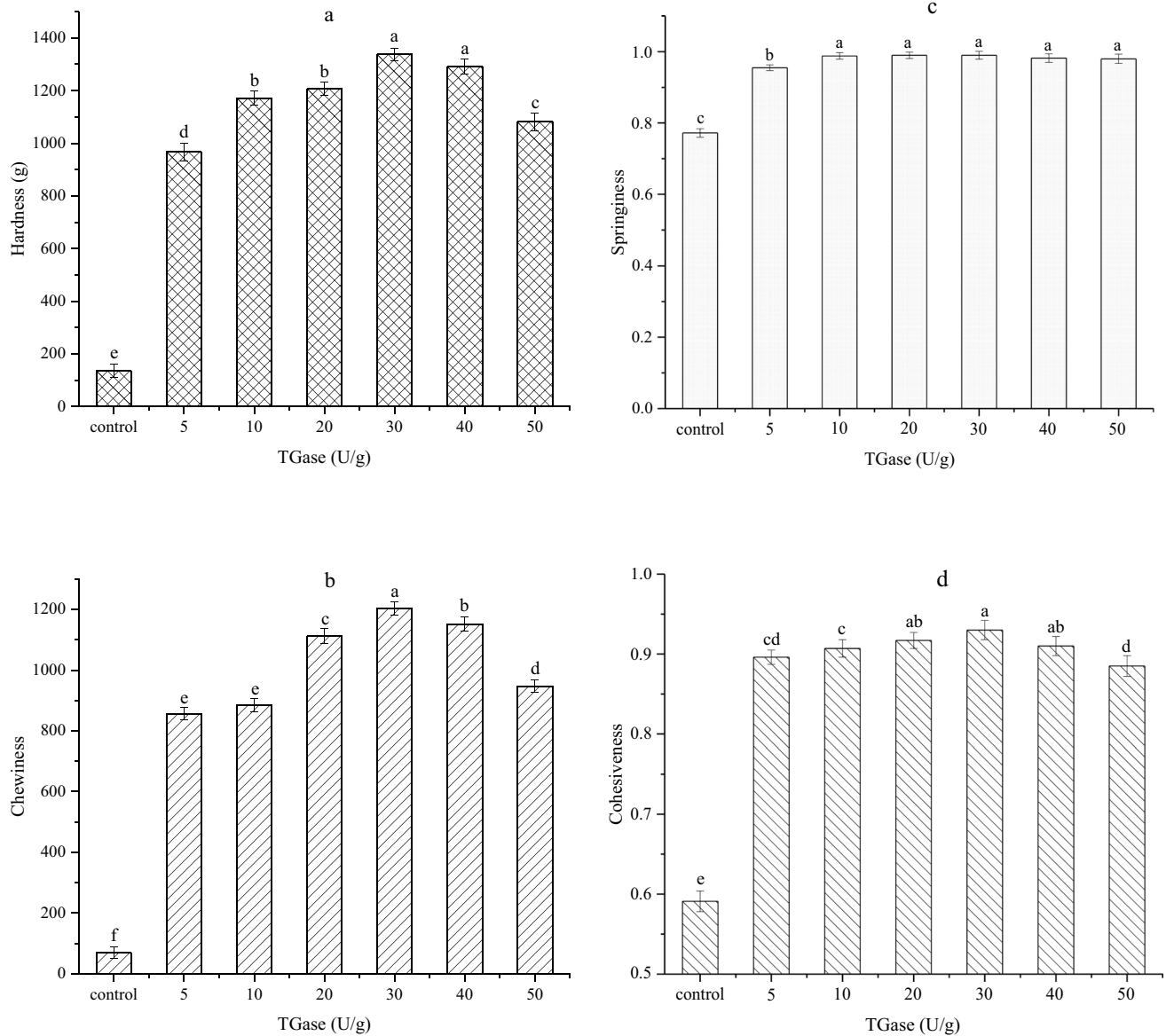


Fig. 8 Changes in hardness (a), chewiness (b), springiness (c) and cohesiveness (d) of MBPG induced by TGase. Data are expressed as mean \pm standard deviation ($n = 3$). Different superscript letters mean

significant differences between values with different TGase concentration ($P < 0.05$)

Fig. 8. The hardness, chewiness, springiness and cohesiveness of TGase-induced MBPG were higher than that of the control, suggesting that TGase improved the textural properties of MBPG. The hardness, chewiness, springiness and cohesiveness of MBPG were enhanced firstly from 135.49 g to 1337.59 g, 69.77 to 1111.43, 0.87 to 0.99 and 0.59 to 0.93 as TGase concentration increased from 0 U/g to 30 U/g, and then decreased sequentially from 1337.59 g to 1080.94 g, 1111.43 to 946.97, 0.99 to 0.98 and 0.93 to 0.89 with increasing TGase concentration from 30 U/g to 50 U/g, respectively. The improved textural properties of MBPG could be explained by the formation of TGase-induced

ϵ -(γ -glutamine)-lysine covalent cross-linking, resulting in Gln-Lys isopeptide bonds that are approximately 20 times stronger than non-covalent bonds [19]. However, TGase concentration beyond 30 U/g declined the textural properties of MBPG. It was possible that too strong TGase concentration led to excessive covalent cross-linking, which prevented intermolecular aggregation and thus weakened the textural properties of MBPG [17]. Similarly, Alavi et al. [49] manifested that formation of covalent cross-linking catalyzed by TGase and the formation of disulfide bonds were corresponding to a considerably increase in hardness, cohesiveness, and chewiness of mixed egg white protein and

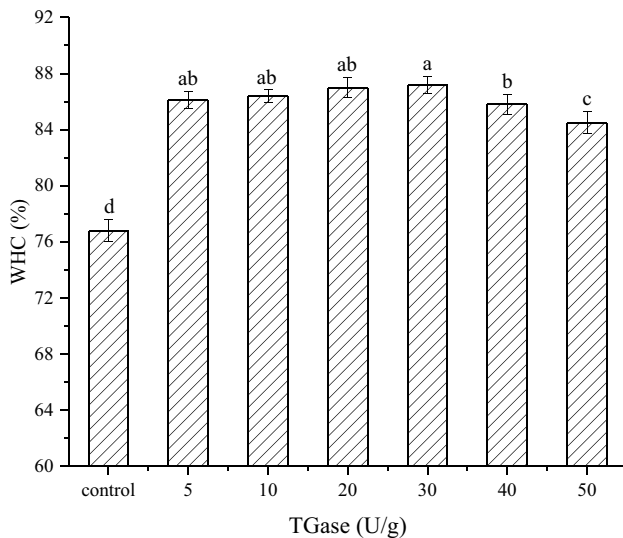


Fig. 9 Changes in WHC of MBPG induced by TGase. Data are expressed as mean \pm standard deviation ($n = 3$). Different superscript letters mean significant differences between values with different TGase concentration ($P < 0.05$)

hempseed protein isolate gel ($P < 0.05$). Moreover, the hardness of casein-cannabis seed protein gels reached a maximum value of 281.99 N at TGase concentration of 30 U/g, which was consistent with our results [32].

WHC Analysis

WHC can reflect the ability of protein-water interactions in the protein gel network, which is a particularly important quality attribute of gels [28]. The effect of TGase on WHC of MBPG is presented in Fig. 9. WHC of MBPG firstly raised from 76.8% to 87.0%, and then dropped from 87.0% to 83.5% with the increase of TGase concentration from 0 U/g to 50 U/g. When TGase concentration was up to 30 U/g, WHC of TGase-induced MBPG reached maximum of 87.0%. These data indicated that TGase improved WHC of MBPG. The more covalent cross-linking between glutamine and lysine residues of MBP induced by TGase formed a dense gel network structure, thus generated better WHC [27]. However, TGase concentration greater than 30 U/g decreased WHC of MBPG. This was because excessive cross-linking interfered with the formation of ordered MBPG matrix [32]. Similar results were observed by Zhou et al. [32], who found that casein-hempseed protein gels showed the highest WHC at 30 U/g TGase, indicating the formation of the densest gel network catalyzed by TGase. Yu et al. [26] observed that compared with the control group, WHC of surimi gel added with 0.1–0.5% TGase was significantly enhanced ($P < 0.05$) with the highest WHC of 78.31% at 0.4% TGase.

Conclusion

The present study illustrated that TGase treatment had the significant effect on structure and gelation properties of MBPG. The change in protein secondary structure of MBPG might be that the formation of macromolecular polymers catalyzed by TGase led to the breaking and reconnection of hydrogen bonds, which were the main force maintaining the protein secondary structure. Moreover, the protein bands of TGase-induced MBPG became shallow or disappeared, especially the 50.1 kDa band, which was related to the covalent cross-linking catalyzed by TGase to form a high molecular weight polymer (>106.3 kDa). Intermolecular forces included ionic bonds, hydrogen bonds, hydrophobic interaction and disulfide bonds, among which hydrophobic interaction and disulfide bonds were the main interaction forces for MBPG network. TGase-catalyzed covalent cross-linking of protein molecules and free sulfhydryl groups formed macromolecular polymers to bury hydrophobic groups, thereby weakening the hydrophobic interactions of MBPG. Therefore, the covalent cross-linking and the enhancement of disulfide bonds of TGase-induced MBPG resulted in a more compact network structure with smaller and more uniform pores, improving the storage modulus (G'), hardness, chewiness, springiness, cohesiveness and WHC of MBPG. However, excessive cross-linking caused by excessive TGase concentration (>30 U/g) destroyed the uniformity and density of network structure, accompanied by decreased G' , hardness, chewiness, springiness, cohesiveness and WHC.

Author Contributions Rui-Xue Wang: Writing-original draft. Ying-Qiu Li: Conceptualization, Methodology, Funding acquisition. Rui-Xue Wang, Gui-Jin Sun, Chen-Ying Wang, Yan Liang, Dong-Liang Hua, Lei Chen and Hai-Zhen Mo: Investigation. Rui-Xue Wang, Gui-Jin Sun and Chen-Ying Wang: Formal analysis.

Funding This work was supported by Pilot project of science, education and industrialization: major innovation project, exploitation of key technology and demonstration of industrialization for healthy food [2022JBZ01-08]; Science and Technology Cooperation Project of Shandong Province and Chongqing Municipality [2021LYXZ018]; Key Plan of Studying and Developing (Major scientific and technological innovation project) in Shandong Province, China [2020CXGC010604]; Project of postgraduate cultivation, achievement of excellent postgraduate, study and practice of multidimensional cultivation for innovative ability of food specialty postgraduate [24221515]; National Natural Science Foundation of China [31371839]; National Science Foundation of Shandong Province, China [Grant No. ZR2020QC221]; National Natural Science Foundation of China [Grant No. 32201970].

Declarations

Conflict of Interest The authors confirm that they have no conflicts of interest with respect to the work described in this manuscript

References

1. A.C. Alves, G.M. Tavares, *Food Hydrocoll.* **97**, 105171 (2019)
2. F.-F. Liu, Y.-Q. Li, C.-Y. Wang, Y. Liang, X.-Z. Zhao, J.-X. He, H.-Z. Mo, *Food Chem.* **393**, 133397 (2022)
3. J. Xie, M. Du, M. Shen, T. Wu, L. Lin, *Food Chem.* **270**, 243 (2019)
4. N. Gupta, N. Srivastava, S.S. Bhagyawant, *PLoS ONE* **13**, e0191265 (2018)
5. F.-F. Liu, Y.-Q. Li, C.-Y. Wang, X.-Z. Zhao, Y. Liang, J.-X. He, H.-Z. Mo, *Process Biochem.* **111**, 274 (2021)
6. Z. Zhong, Y.L. Xiong, *Ultrason. Sonochem.* **62**, 104908 (2020)
7. Y. Nie, Y. Liu, J. Jiang, Y.L. Xiong, X. Zhao, *Food Hydrocoll.* **129**, 107607 (2022)
8. Q. Cui, G. Wang, D. Gao, L. Wang, A. Zhang, X. Wang, N. Xu, L. Jiang, *Process Biochem.* **91**, 104 (2020)
9. B. Herranz, C.A. Tovar, A.J. Borderias, H.M. Moreno, *Innovative Food Sci. Emerging Technol.* **20**, 24 (2013)
10. N. Chen, M. Zhao, C. Chassenieux, T. Nicolai, *Food Hydrocoll.* **70**, 88 (2017)
11. O. Nivala, E. Nordlund, K. Kruus, D. Ercili-Cura, *LWT-Food. Sci. Technol.* **139**, 110517 (2021)
12. T.G. Kudre, S. Benjakul, *Food Biophys.* **8**, 240 (2013)
13. Y. Li, S. Damodaran, *Food Chem.* **221**, 1151 (2017)
14. M. Jin, Q. Zhong, *J. Food Eng.* **115**, 33 (2013)
15. S.B.M. Yasir, K.H. Sutton, M.P. Newberry, N.R. Andrews, J.A. Gerrard, *Food Chem.* **104**, 1491 (2007)
16. X.D. Sun, S.D. Arntfield, *Food Hydrocoll.* **25**, 25 (2011)
17. M.H. Norziah, A. Al-Hassan, A.B. Khairulnizam, M.N. Mordi, M. Norita, *Food Hydrocoll.* **23**, 1610 (2009)
18. N.K.K. Kamizake, M.M. Gonçalves, C.T.B.V. Zaia, D.A.M. Zaia, *J. Food Compos. Anal.* **16**, 507 (2003)
19. X. Wen, F. Jin, J.M. Regenstien, F. Wang, *Food Biosci.* **26**, 15 (2018)
20. Y. Li, X. Li, J. Wang, C. Zhang, H. Sun, C. Wang, X. Xie, *Food Biophys.* **9**, 169 (2014)
21. X. Liang, C. Ma, X. Yan, H. Zeng, D.J. McClements, X. Liu, F. Liu, *Food Hydrocoll.* **102**, 105569 (2020)
22. D. Jia, Q. Huang, S. Xiong, *Food Chem.* **196**, 1180 (2016)
23. M.A.K. Markwell, S.M. Haas, L.L. Bieber, N.E. Tolbert, *Anal. Biochem.* **87**, 206 (1978)
24. M.R. Salahi, S.M.A. Razavi, M. Mohebbi, *Food Biophys.* **17**, 635 (2022)
25. S. Patole, L. Cheng, Z. Yang, *Food Biophys.* **17**, 314 (2022)
26. N. Yu, F. Yang, H. Gong, J. Zhou, C. Jie, W. Wang, X. Chen, L. Sun, *J. Food Eng.* **323**, 111006 (2022)
27. Q. Fang, L. Shi, Z. Ren, G. Hao, J. Chen, W. Weng, *LWT-Food. Sci. Technol.* **146**, 111513 (2021)
28. M. Zhang, Y. Yang, N.C. Acevedo, *Food Chem.* **318**, 126421 (2020)
29. K. Agyare, Y. Xiong, K. Addo, *Food Chem.* **S0308814607009545** (2007)
30. X.-S. Qin, S.-Z. Luo, J. Cai, X.-Y. Zhong, S.-T. Jiang, Y.-Y. Zhao, Z. Zheng, *Ultrason. Sonochem.* **31**, 590 (2016)
31. C.-H. Tang, X. Sun, S.-W. Yin, C.-Y. Ma, *Food Res. Int.* **41**, 941 (2008)
32. X. Zhou, Y. Zheng, Y. Zhong, D. Wang, Y. Deng, *Food Chem.* **383**, 132366 (2022)
33. Z.-Z. Hu, X.-M. Sha, T. Huang, L. Zhang, G.-Y. Wang, Z.-C. Tu, *Food Chem.* **348**, 129093 (2021)
34. X. Deng, Y. Ma, Y. Lei, X. Zhu, L. Zhang, L. Hu, S. Lu, X. Guo, J. Zhang, *Ultrason. Sonochem.* **76**, 105659 (2021)
35. K. Yokoyama, N. Nio, Y. Kikuchi, *Appl. Microbiol. Biotechnol.* **64**, 447 (2004)
36. N. Aktas, B. Kiliç, *LWT-Food. Sci. Technol.* **38**, 815 (2005)
37. Q.-Q. Zhang, Inner Mongol University of Technology (China). (2021)
38. A.M. Herrero, M.I. Cambero, J.A. Ordóñez, L. de la Hoz, P. Carmona, *Food Chem.* **109**, 25 (2008)
39. K. Luo, S. Liu, S. Miao, B. Adhikari, X. Wang, J. Chen, *J. Food Eng.* **263**, 280 (2019)
40. K. Wang, S. Luo, J. Cai, Q. Sun, Y. Zhao, X. Zhong, S. Jiang, Z. Zheng, *Food Chem.* **197**, 168 (2016)
41. Y.-Y. Wang, J.-K. Yan, Y. Ding, M.T. Rashid, H. Ma, *LWT-Food. Sci. Technol.* **150**, 111922 (2021)
42. A.S. Eissa, S.A. Khan, *Food Hydrocoll.* **20**, 543 (2006)
43. Y. Hu, W. Liu, C. Yuan, K. Morioka, S. Chen, D. Liu, X. Ye, *Food Chem.* **176**, 115 (2015)
44. S. Qian, P. Dou, J. Wang, L. Chen, X. Xu, G. Zhou, B. Zhu, N. Ullah, X. Feng, *Food Chem.* **349**, 129066 (2021)
45. C. Chen, P. Wang, N. Zhang, W. Zhang, F. Ren, *LWT-Food. Sci. Technol.* **103**, 53 (2019)
46. G. Oliver, P. E. Pritchard, in *Food Colloids and Polymers*, edited by E. Dickinson and P. Walstra (Woodhead Publishing, 2005), pp. 255-259
47. X.D. Sun, S.D. Arntfield, *J. Food Eng.* **107**, 226 (2011)
48. T. Xing, Y. Xu, J. Qi, X. Xu, X. Zhao, *Food Chem.* **347**, 129031 (2021)
49. F. Alavi, Z. Emam-Djomeh, L. Chen, *Food Hydrocoll.* **107**, 105960 (2020)

Publisher's Note Springer Nature remains neutral with regard to jurisdictional claims in published maps and institutional affiliations.

Springer Nature or its licensor (e.g. a society or other partner) holds exclusive rights to this article under a publishing agreement with the author(s) or other rightsholder(s); author self-archiving of the accepted manuscript version of this article is solely governed by the terms of such publishing agreement and applicable law.